frontiers | Frontiers in Pharmacology

ORIGINAL RESEARCH
published: 11 July 2022
doi: 10.3389/fphar.2022.935588

A Selective Adenylyl Cyclase 1 Inhibitor Relieves Pain Without Causing Tolerance

*Gianna Giacoletti[1], Tatum Price[1], Lucas V. B. Hoelz[2], Abdulwhab Shremo Msdi[1], Samantha Cossin[1], Katerina Vazquez-Falto[1], Tácio V. Amorim Fernandes[2,3], Vinícius Santos de Pontes[2], Hongbing Wang[4], Nubia Boechat[2], Adwoa Nornoo[1] and Tarsis F. Brust[1]**

[1]Department of Pharmaceutical Sciences, Lloyd L. Gregory School of Pharmacy, Palm Beach Atlantic University, West Palm Beach, FL, United States, [2]Laboratório de Síntese de Fármacos—LASFAR, Instituto de Tecnologia em Fármacos, Farmanguinhos—FIOCRUZ, Fundação Oswaldo Cruz, Rio de Janeiro, Brazil, [3]Instituto Nacional de Metrologia, Qualidade e Tecnologia—INMETRO, Rio de Janeiro, Brazil, [4]Department of Physiology, Michigan State University, East Lansing, MI, United States

OPEN ACCESS

Edited by:
Manuela Marcoli,
University of Genoa, Italy

Reviewed by:
Victor Ruiz-Velasco,
The Pennsylvania State University, United States
J. Adolfo García-Sáinz,
Universidad Nacional Autónoma de México, Mexico

***Correspondence:**
Tarsis F. Brust
tbrust@atyrpharma.com

Specialty section:
This article was submitted to Experimental Pharmacology and Drug Discovery, a section of the journal Frontiers in Pharmacology

Received: 04 May 2022
Accepted: 20 June 2022
Published: 11 July 2022

Citation:
Giacoletti G, Price T, Hoelz LVB, Shremo Msdi A, Cossin S, Vazquez-Falto K, Amorim Fernandes TV, Santos de Pontes V, Wang H, Boechat N, Nornoo A and Brust TF (2022) A Selective Adenylyl Cyclase 1 Inhibitor Relieves Pain Without Causing Tolerance. Front. Pharmacol. 13:935588. doi: 10.3389/fphar.2022.935588

Among the ten different adenylyl cyclase isoforms, studies with knockout animals indicate that inhibition of AC1 can relieve pain and reduce behaviors linked to opioid dependence. We previously identified ST034307 as a selective inhibitor of AC1. The development of an AC1-selective inhibitor now provides the opportunity to further study the therapeutic potential of inhibiting this protein in pre-clinical animal models of pain and related adverse reactions. In the present study we have shown that ST034307 relives pain in mouse models of formalin-induced inflammatory pain, acid-induced visceral pain, and acid-depressed nesting. In addition, ST034307 did not cause analgesic tolerance after chronic dosing. We were unable to detect ST034307 in mouse brain following subcutaneous injections but showed a significant reduction in cAMP concentration in dorsal root ganglia of the animals. Considering the unprecedented selectivity of ST034307, we also report the predicted molecular interaction between ST034307 and AC1. Our results indicate that AC1 inhibitors represent a promising new class of analgesic agents that treat pain and do not result in tolerance or cause disruption of normal behavior in mice. In addition, we outline a unique binding site for ST034307 at the interface of the enzyme's catalytic domain.

Keywords: adenylyl cyclase, pain, analgesia, AC1, tolerance

1 INTRODUCTION

Adenylyl cyclases (ACs) are the enzymes responsible for catalyzing the conversion of adenosine triphosphate (ATP) into cyclic adenosine monophosphate (cAMP) (Cooper and Crossthwaite, 2006; Dessauer et al., 2017). ACs integrate signaling from a large range of proteins and ions, including G protein-coupled receptors (GPCRs), protein kinases, and calcium, to name a few. There are ten different isoforms of ACs, nine of them are present in the cellular membrane and one is soluble. Each AC isoform has a specific expression pattern, which is related to a specific set of physiological functions (Ostrom et al., 2022). AC isoforms also display a unique set of regulatory properties that result in differences in how the isoforms are modulated by different types of G proteins, protein kinases, and ions (Cooper and Crossthwaite, 2006; Dessauer et al., 2017).

AC1 is part of the group of ACs that are activated by calcium through calmodulin (Masada et al., 2012). Additional regulatory properties of AC1 include inhibition by $G\alpha_{i/o}$ and $G\beta\gamma$ subunits of G proteins and activation by $G\alpha_s$ and the small molecule forskolin (Brust et al., 2017; Dessauer et al., 2017). AC1 has also been shown to undergo $G\alpha_{i/o}$-coupled receptor-mediated superactivation (Cumbay and Watts, 2001; Brust et al., 2015; Brust et al., 2017). The expression pattern of AC1 is consistent with the physiological functions that have been associated with this AC isoform. AC1 transcripts are found in the dorsal root ganglion (DRG), spinal cord, and anterior cingulate cortex (ACC), and a role for this cyclase in pain and nociception has been suggested (Wei et al., 2006; Xu et al., 2008; Johnson et al., 2020). In fact, AC1 knockout (KO) mice display a reduction in typical behaviors that are induced by inflammatory and neuropathic pain, compared to wild-type mice (Wei et al., 2002; Vadakkan et al., 2006; Xu et al., 2008). These studies encouraged the pursuit and discovery of novel compounds that can selectively inhibit AC1 activity as potential novel pain-relieving therapeutics (Brand et al., 2013; Brust et al., 2017; Kaur et al., 2018).

AC1 transcripts are also found in the hippocampus, a brain region linked to learning and memory (Wong et al., 1999). Notably, AC8, another calcium/calmodulin-activated isoform, is also highly expressed in the hippocampus (Wang et al., 2003; Dessauer et al., 2017). Previous studies with single and double AC1/AC8 KO mice have indicated that some functions of AC1 and AC8 related to learning and memory are redundant (Wong et al., 1999). Specifically, AC1/AC8 double KO mice display impaired long-term memory in contextual learning and passive avoidance assays, whereas individual KO of each isoform separately results in wild-type-like behaviors (Wong et al., 1999). However, each isoform also appears to have specific functions. While less severe deficits are observed in AC1-KO mice compared to the AC1/AC8 double KO, the former still displays reduced long-term potentiation (LTP) in the hippocampus and impairments in certain recognition memory as well as spatial and avoidance learning tasks (Shan et al., 2008; Zheng et al., 2016). Those studies highlight the importance of selectivity for AC1 inhibition versus AC8 for a novel compound to treat pain, but do not exclude the possibility of adverse effects that may result from selective AC1 inhibition in the hippocampus.

We have recently reported the discovery of ST034307, a small molecule inhibitor of AC1 that is selective for AC1 inhibition versus all other membranous AC isoforms, including AC8 (Brust et al., 2017). Our previous study focused on the characterization of ST034307 at the molecular level, showing that the compound is a potent, highly selective, and direct AC1 inhibitor. Moreover, ST034307 was also analgesic in a mouse model of Complete Freund's Adjuvant (CFA)-induced allodynia (Brust et al., 2017). The present study represents a pre-clinical study with ST034307 to determine the potential of this class of compounds as novel analgesic agents. We compared the compound with morphine in mouse models of pain-induced and pain-depressed behaviors and also showed that the compound appears to be restricted to the periphery following subcutaneous injections and reduces cAMP concentration in mouse DRG. Further, we showed that ST034307 does not induce analgesic tolerance or cross-tolerance with morphine. Finally, we expanded our previous mechanistic findings by modeling how the interaction of ST034307 with AC1 happens, this may aid future medicinal chemistry studies pursuing selective modulators of AC1.

2 MATERIALS AND METHODS

2.1 Experimental Design

The main goal of the present study was to determine the potency and efficacy of the AC1 selective inhibitor ST034307 in mouse models of pain and innate behavior. Male mice were used as research subjects and sample sizes for the different experiments were determined using power analyses from preliminary experiments following the guidelines of Palm Beach Atlantic University's Institutional Animal Care and Use Committee (IACUC) to attempt to minimize the numbers of animals used. Instances where the number of animals per group vary in an experiment were the result of additional animals being required for proper blinding when a drug dose was added. All animals were randomized to treatments and experimenters performing behavioral measurements and injections were blinded to all compound treatments and doses.

2.2 Materials

ST034307 (6-Chloro-2-(trichloromethyl)-4H-1-benzopyran-4-one) was purchased from Tocris Bioscience and morphine sulphate from Spectrum Laboratory Products. Acetic acid, lactic acid, Tween 80, and formaldehyde were from Sigma-Aldrich. Dimethyl sulfoxide (DMSO) and 0.9% sterile saline were from Fisher Scientific. ST034307 and morphine were prepared in a vehicle consisting of dimethyl sulfoxide (DMSO), Tween 80, and milli-Q water (1:1:8). Specifically, ST034307 was first dissolved in DMSO and sonicated in a 50°C water bath for 15 min. Next, Tween 80 was added, the solution was vortexed, and the sonication was repeated. Warm (37°C) milli-Q water was added and the solution was vortexed immediately before injections. While morphine is also soluble in aqueous solutions, such as saline, we chose to dilute it in the same vehicle as ST034307 to avoid having to add an additional vehicle control condition to our experiments. These procedures reduced the number of animals required in all *in vivo* experiments performed in the study. Acetic acid, lactic acid, and formalin were diluted in 0.9% sterile saline.

2.3 Study Approval

All experimental procedures involving mice adhered to the National Institutes of Health Animal Care guidelines and were approved by Palm Beach Atlantic University's IACUC (West Palm Beach, FL—protocol number 2020-01AMOUSE approved on 10 January 2020).

2.4 Animals

Male C57BL/6J mice were purchased from Charles Rivers Laboratories. This particular strain is commonly used in

studies related to analgesic agents (Brust et al., 2016; Grim et al., 2020; Pantouli et al., 2021) and provides a way of comparing the activity of ST034307 with other compounds, given that morphine was used as a positive control. AC1-KO mice were created as previously described and propagated using homozygous breeding using the C57BL/6J background (Zheng et al., 2016). Mice were housed in groups (2-5 per cage) in cages covered with filter tops (micro barrier top from Allentown), in a temperature-controlled room under a 12-h light/dark cycle. Animals had ad libitum access to water and food, as well as nesting material made from pulped virgin cotton fiber (nestlets from Lab Supply) for enrichment. Corn cob bedding (1/4") was used for bedding. Mice between 2 and 5 months of age were used for experiments and were dosed subcutaneously with 10 µl/g of ST034307, morphine, or vehicle solutions. After each experiment, mice were humanely euthanized via cervical dislocation under isoflurane anesthesia (open drop method).

2.5 Formalin-Induced Paw Licking

The formalin-induced paw licking assay was conducted similarly to previously described (Pantouli et al., 2021). Briefly, mice were acclimated to clear testing cylinders for 45 min. Next, mice were injected subcutaneously with compounds or vehicle solutions and returned to acrylic cylinders for 15 min. Mice were then injected into their right hind paw with 25 µl of 5% formalin using a 25 µl Hamilton syringe and a 30-gauge needle. Mice were immediately returned to the testing cylinders, and paw licking time was recorded in 5-min intervals for 40 min. The experiment was divided into two different phases. The first represents the time spent licking between 0 and 10 min, the second represents the time spent licking between 16 and 40 min.

2.6 Acid-Induced Writhing

For the acid-induced writhing assay, mice were acclimated to clear testing cylinders for 45 min. Next, mice were injected subcutaneously with compounds or vehicle solutions and returned to acrylic cylinders for 15 min. Mice were then injected intraperitoneally with 0.75% acetic acid (10 µl/g), returned to the testing cylinders, and the number of abdominal constrictions (stretching movements of the body as a whole, including the hind paws) was counted in 5-min intervals for 30 min as previously described (Tarselli et al., 2011). For the tolerance assay, mice were injected subcutaneously with either 100 mg/kg morphine or 30 mg/kg ST034307 (solubility issues prevented the use of higher doses) once a day for four or 8 days. Three hours after the last injection at day four or day eight, acid-induced writhing assays were performed.

2.7 Nesting

The mouse nesting assay was adapted from methods previously described (Negus et al., 2015). Mice were single housed and acclimated to their new home cage for 3 days. During the following 3 days, mice underwent one nesting session (as described below) per day to acclimate them to handling, the experimental procedure, and the testing room. The last acclimation session included a subcutaneous injection (for compound-inhibited nesting) or a subcutaneous injection and an intraperitoneal injection (for acid-depressed nesting) with 0.9% saline. On the day after the third acclimation session, mice were injected subcutaneously with compounds or vehicle and returned to their respective home cages for 10 min. Mice were transferred to a transfer cage (<1 min) and nestlets we placed in each of the 6 different zones of the home cage as previously described (Negus et al., 2015). Mice were either returned to their home cages (compound-inhibited nesting) or injected intraperitoneally (10 µl/g) with 1% lactic acid (acid-depressed nesting) and returned to their home cages for nesting periods. Nesting was scored as the number of zones cleared over time.

2.8 Pharmacokinetic Studies

The disposition of ST034307 was studied in male C57BL/6J mice following a single subcutaneous injection (10 mg/kg). Mice were humanely euthanized via decapitation under isoflurane anesthesia (open drop method). Subsequently, brain and blood samples were collected at 5-, 25-, 45-, 60-, 120-, and 240-min post-injection. Blood was centrifuged, plasma collected and stored at −80°C. The analyses of the samples were conducted in the Drug Metabolism and Pharmacokinetics Core at Scripps Research. Brain samples were homogenized with water to form a slurry. ST0304307 was extracted from plasma and brain slurry on solid-supported liquid-liquid extraction cartridges (HyperSep™, SLE, 1 g/6 ml, Thermo Scientific) and the resultant extract was assayed for ST034307 by tandem mass spectroscopy coupled to HPLC (SCIEX 6500). The lowest limits of quantitation were 10 ng/ml (34 nM) and 6 ng/ml (20 nM) for plasma and brain, respectively. A plot of plasma ST0304307 concentration versus time was constructed and analyzed for non-compartmental pharmacokinetic parameters - half-life, volume of distribution and clearance (Phoenix, Pharsight, Certara Inc.).

2.9 Cyclic AMP Production in Mouse DRG

Male C57BL/6J mice were injected subcutaneously with 10 mg/kg ST034307 or vehicle. Mice were humanely euthanized *via* decapitation under isoflurane anesthesia (open drop method) 90 min after the injection. DRGs (approximately C5 to L3) were dissected as previously described (Sleigh et al., 2020), frozen in liquid N_2, and stored in a −80°C freezer until used. On assay day, DRGs from a ST034307-injected mouse and its vehicle-matched control were thawed on ice. Membrane buffer (50 mM HEPES, pH 7.4) was added and samples were homogenized using a tissue tearor. Next, samples were subjected to glass-on-glass dounce homogenization. Homogenates were centrifuged at 500 x g for 5 min at 4°C. The supernatant was collected and centrifugation was repeated until no visible pellet remained. Homogenates were plated in a low-volume 348 well plate at a protein concentration of 100 ng/well. Stimulation buffer (final well concentrations: 50 mM HEPES pH 7.4, 10 mM $MgCl_2$, 0.2 mM ATP, 10 uM GTP, 1% DMSO, 50 mM NaCl, 500 µM 3-isobutyl-1-methylxanthine, and 0.5 mg/ml bovine serum albumin) was added and the plate was incubated at room temperature for 45 min. cAMP concentrations were measured using Cisbio's dynamic 2 kit (Cisbio Bioassays) according to the manufacturer's instructions.

2.10 Molecular Docking

2.10.1 Construction of the AC1 Model

The AC1 model was constructed through ab-initio and threading methods on I-Tasser server, considering as input the sequences Phe291-Pro478 and Leu859-1058, registered under the UniProtKB ID Q08828 (Yang and Zhang, 2015; UniProt, 2021). The globular domain regions were identified using both Pfam and UniProtKB feature viewer, being selected for further refining (Mistry et al., 2021). Local sequence alignments with NCBI's BLAST+ were made between the Q08828 and those from Protein Data Bank (PDB) deposited structures to find experimentally solved structures with magnesium ions, ATP, and $G\alpha_s$ on their respective sites (Altschul et al., 1990; Berman et al., 2002). Thus, using molecular superpositions on VMD 1.9.3, the cofactors and ligands were extracted from the structure registered as 1CJK on PDB, while $G\alpha_s$ was extracted from the structure registered as 6R3Q, and positioned into the AC1 model (Humphrey et al., 1996). MODELLER 9.25-1 was then used to run 100 cycles of structural optimizations with molecular dynamics, simulated annealing, and conjugated gradient (Sali and Blundell, 1993). The generated structures were ranked by DOPE-Score and the best model was selected. To verify the structural quality of the best AC1 model built, the structure was submitted to the SAVES server, where two programs were selected, PROCHECK (**Supplementary Figures. S1–S3**) and VERIFY 3D (**Supplementary Figure S4**), and to the Swiss-PROT server, using QMEANDisCo algorithm (**Supplementary Figure S5**) (Colovos and Yeates, 1993; Laskowski et al., 1993; Studer et al., 2020).

2.10.2 Preparation of the ST034307 Structure

ST034307 was constructed and optimized with the HF/6-31G(d) level of theory using the SPARTAN′16 program (Wavefunction, Inc.).

2.10.3 Docking Using GOLD 2020.3.0 (Genetic Optimization for Ligand Docking)

The molecular docking simulation using the GOLD program was carried out using automatic genetic algorithm parameters settings for the population size, selection-pressure, number of islands, number of operations, niche size, and operator weights (migration, mutation, and crossover) (Jones et al., 1997). The search space was a 40 Å radius sphere from the 66.215, 105.567, and 81.040 (x, y, and *z* axes, respectively) coordinates. The scoring function used was ChemPLP, which is the default function for the GOLD program. Thus, the pose with the most positive score (the best interaction) was extracted for further analysis.

2.10.4 Docking Using AutoDock Vina 1.1.2

The PDBQT-formatted files for the AC1 model and ST034307 structure were generated using AutoDock Tools (ADT) scripts (Trott and Olson, 2010). Using the AutoDock Vina program, the grid size was set to 65.172 Å × 77.050 Å × 73.559 Å for x, y, and *z* axes, respectively, and the grid center was chosen using 66.215 (x), 105.567 (y), and 81.040 (z) as coordinates. Each docking run used an exhaustiveness setting of 16 and an energy range of 3 kcal/mol. Consequently, the pose with the lowest energy was extracted for interaction analysis.

2.11 Data and Statistical Analyses

All statistical analyses were carried out using GraphPad Prism 9 software (GraphPad Software Inc.). Data normalization and nonlinear regressions were carried out similarly to previously described (Grim et al., 2020). For normalizations (representing a rescaling of the *Y* axis for enhanced clarity), the maximal possible effect was set as 100% (zero for formalin-induced paw licking and acid-induced writhing, and five for acid-depressed nesting) and the response to vehicle's average as 0%. For compound-inhibited nesting, the response from vehicle's average was defined as 100% and zero to 0%. Normalized data was fitted to three-parameter nonlinear regressions with the top constrained to 100% and the bottom to 0% (except for the cases where ST034307 did not reach a full response, where no top constrain was set—**Figure 2C**, **Figure 3F**). The constrains were done in order to reduce the number of animals used in the experiments and based on the assumption that lower compound doses would not cause an effect lower than the effect of vehicle and the fact that each experiment performed has a ceiling effect (e.g., the lowest amount of time a mouse can lick its paw is zero). All statistical analyses of mouse behavioral responses were performed using raw experimental data (without normalization). For the DRG studies, a matched vehicle control was included with each experiment and cAMP concentration was normalized to that control. Therefore, a one sample T test was carried out to compare the normalized values obtained from mice injected with ST034307 with 100%. T tests with Welch's correction were used for comparisons between genotypes, one-way ANOVAs for comparisons within groups, and two-way ANOVAs for time-course evaluations. All ANOVAs where F achieved a statistical level of significance ($p < 0.05$) were followed by Dunnett's corrections and significance was set at a $p < 0.05$.

3 RESULTS

3.1 ST034307 Relieves Inflammatory Pain, but Not Acute Nociception in Mice

We have previously shown that intrathecal administration of ST034307 relieves CFA-mediated allodynia in mice (Brust et al., 2017). Here, we used intraplantar formalin injections to the mice's right hind paws and compared the potency of ST034307 with that of morphine (both administered subcutaneously) for diminishing acute nociception and relieving inflammatory pain. The time spent tending to (licking) the injected paw was recorded (**Figures 1A,B**). As indicated by previous studies using AC1-KO mice (Wei et al., 2002), only morphine caused a significant reduction in acute nociception, with an ED_{50} value equal to 5.87 mg/kg [95% CI 0.44 to 8.96] (**Figure 1C**—sum of measurements recorded between 0 and 10 min). No significant effect was observed with ST034307. In contrast, both compounds significantly reduced formalin-induced paw licking in the inflammatory pain phase of the model compared to vehicle and had ED_{50} values equal to

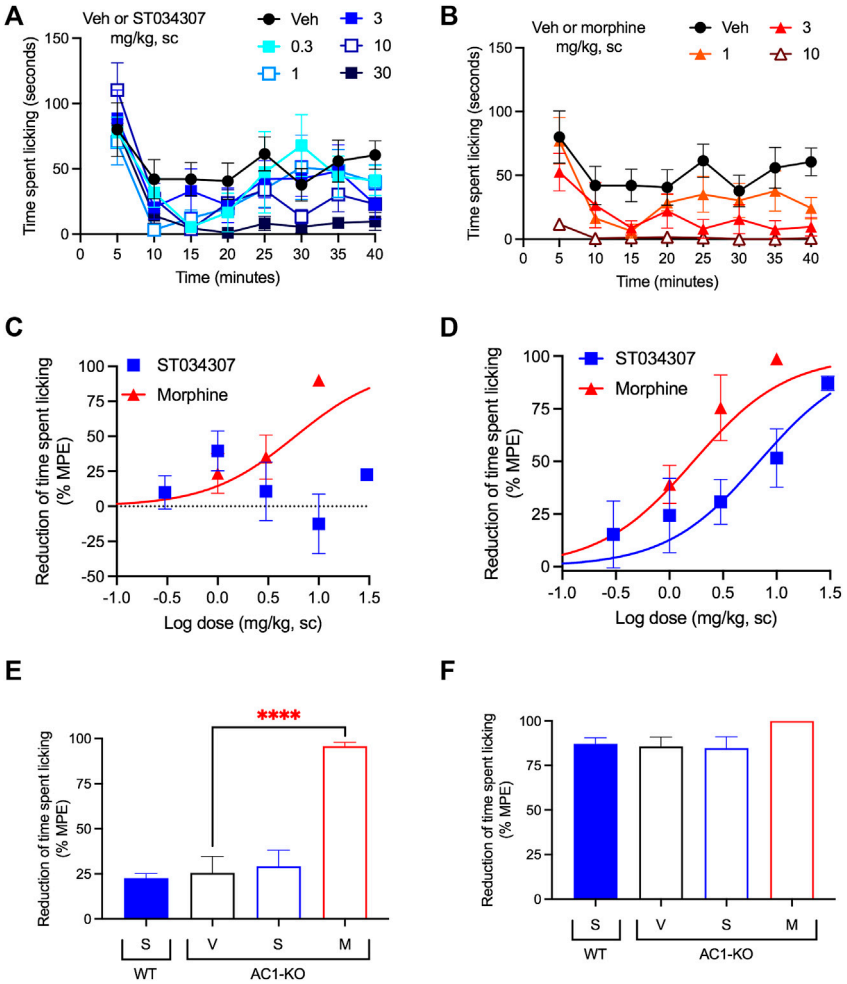

FIGURE 1 | ST034307 relieves inflammatory pain in mice. **(A)** Different doses of ST034307 reduce paw licking behavior caused by an intraplantar injection with 5% formalin. **(B)** Different doses of morphine reduce paw licking behavior caused by an intraplantar injection with 5% formalin. **(C)** Dose-response curves of the sum of time spent licking the paw during the first 10 min of the graphs in **(A)** and **(B)**. Vehicle's response was set as 0% and the maximal possible effect (0) to 100%. **(D)** Dose-response curves of the sum of time spent licking the paw during the period in between minute 16 and minute 40 of the graphs in **(A)** and **(B)**. Vehicle's response was set as 0% and the maximal possible effect (0) to 100%. **(E)** Reduction of time spent licking the injected paw in wild-type (WT) and in AC1-KO mice treated with vehicle (V), 30 mg/kg ST034307 (S), or 10 mg/kg morphine (M) during the first 10 min of the experiment. **(F)** Reduction of time spent licking the injected paw in wild-type (WT) and in AC1-KO mice treated with vehicle (V), 30 mg/kg ST034307 (S), or 10 mg/kg morphine (M) during the period in between minute 16 and minute 40 of the experiment. For E and F vehicle's response in wild-type mice was set to 0% and zero to 100%. Data in all graphs represent the average ±S.E.M., N = 6–8. ****$p < 0.0001$ in one-way ANOVA with Dunnett's test.

6.88 mg/kg [95% CI 0.85 to 14.05] and 1.67 mg/kg [95% CI 0.35 to 2.43] for ST034307 and morphine, respectively (**Figure 1D**—sum of measurements recorded between 16 and 40 min).

Consistent with the results from wild-type mice, AC1-KO mice did not present a reduction of licking during the acute nociception phase of the experiment compared to wild-type mice ($p = 0.2089$ in unpaired t test–**Figure 1E**). In addition, while morphine relieved acute nociception in AC1-KO mice ($p < 0.0001$ in one-way ANOVA), no effects were observed with ST034307 (**Figure 1E**). In contrast, AC1-KO mice displayed a significant reduction of licking in the inflammatory phase of the model, compared to wild-type mice ($p < 0.001$ in unpaired t test–**Figure 1F**). That reduction was similar to the effect 30 mg/kg ST034307 had in wild-type mice. No effects were observed from a dose of 30 mg/kg ST034307 in AC1-KO mice. Morphine (10 mg/kg) had a small effect in the inflammatory phase, but it was not significantly different from vehicle ($p = 0.087$ in one-way ANOVA–**Figure 1F**).

3.2 ST034307 Relieves Visceral Pain and Does Not Induce Analgesic Tolerance in Mice

Visceral pain was induced by an intraperitoneal injection of 0.75% acetic acid. The number of abdominal stretches (writhing) the mice performed over a period of 30 min was recorded (**Figures 2A,B**). Both ST034307 and morphine significantly reduced acid-induced writhing in this model with

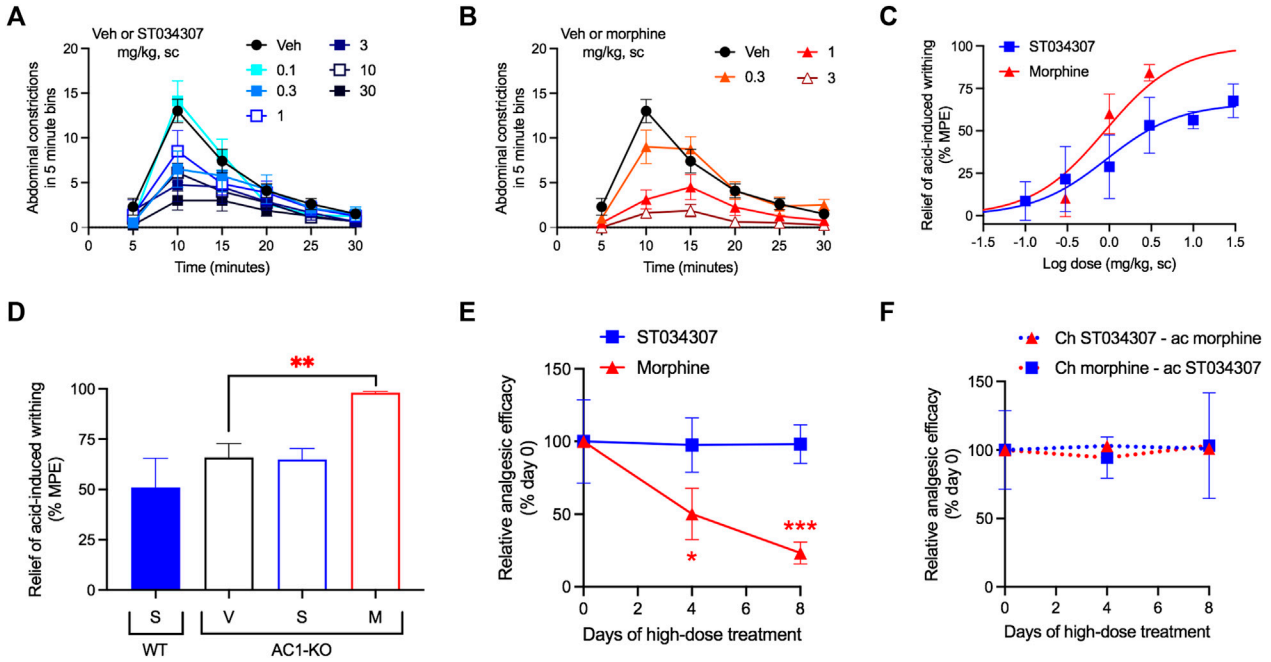

FIGURE 2 | ST034307 relieves visceral pain in mice. **(A)** Different doses of ST034307 reduce the number of abdominal constrictions caused by an intraperitoneal injection with 0.75% acetic acid; N = 8–10. **(B)** Different doses of morphine reduce the number of abdominal constrictions caused by an intraperitoneal injection with 0.75% acetic acid; N = 8–10. **(C)** Dose-response curves of the total number of abdominal constrictions from the graphs in **(A)** and **(B)**. Vehicle's response was set as 0% and the maximal possible effect (0) to 100%. **(D)** Reduction of the total number of abdominal constrictions in wild-type (WT) and in AC1-KO mice treated with vehicle (V), 30 mg/kg ST034307 (S), or 10 mg/kg morphine (M). Vehicle's response in wild-type mice was set as 0% and zero to 100%; N = 5. **(E)** Mice were injected daily with 30 mg/kg ST034307 or 100 mg/kg morphine and on day four or eight acid-induced writhing assays were performed. Mice that chronically received morphine displayed a decrease in efficacy of 3 mg/kg morphine on days four or eight, compared to a group of mice that received vehicle plus 3 mg/kg morphine on day zero. Mice that chronically received ST034307 did not display any changes in efficacy of 10 mg/kg ST034307; N = 5. **(F)** Mice were injected daily with 30 mg/kg ST034307 or 100 mg/kg morphine and on day four or eight acid-induced writhing assays were performed. Mice that chronically received morphine did not display any changes in efficacy with 10 mg/kg ST034307. Mice that chronically received ST034307 did not display any changes in efficacy with 3 mg/kg morphine; N = 5. Data in all graphs represent the average ±S.E.M. $*p < 0.05$, $**p < 0.01$, $***p < 0.001$ in one-way ANOVA with Dunnett's test.

ED_{50} values equal to 0.92 mg/kg [95% CI 0.15 to 4.41] and 0.89 mg/kg [95% CI 0.40 to 1.52], respectively (**Figure 2C**). However, ST034307 did not reach full efficacy at doses up to 30 mg/kg. Similarly, AC1-KO mice also only showed a partial reduction of acid-induced writhing in this model, compared to wild-type mice ($p < 0.001$ in unpaired t test, **Figure 2D**). This response was not enhanced by 10 mg/kg ST034307, but 3 mg/kg morphine caused a significant reduction of acid-induced writhing in AC1-KO mice ($p < 0.01$ in one-way ANOVA—**Figure 2D**).

Mice treated chronically with morphine display analgesic tolerance. Tolerance is expressed through the gradual loss in efficacy of a compound's dose over time (Raehal et al., 2011). After 4 days of daily subcutaneous injections with 100 mg/kg morphine, the efficacy of a 3 mg/kg dose of morphine decreased by nearly half (**Figure 2E**). At day eight, morphine's efficacy was nearly 20% of its initial response (**Figure 2E**). In contrast, daily subcutaneous injections with 30 mg/kg ST034307 (highest dose we were able to inject chronically due to solubility) caused no decrease in the analgesic efficacy of a 10 mg/kg ST034307 dose at day four or day eight (**Figure 2E**). Notably, no cross-tolerance was developed between the two compounds (**Figure 2F**). Mice treated daily with 100 mg/kg morphine were still fully responsive to 10 mg/kg ST034307 at days four and eight; and mice treated daily with 30 mg/kg ST034307 were also fully responsive to 3 mg/kg morphine at days four and eight (**Figure 2F**).

3.3 ST034307 Promotes Analgesia in the Absence of Disruptions in the Mouse Nesting Model

Nesting is an innate mouse behavior that can be disrupted by a number of different stimuli (Negus et al., 2015). Drugs, stress, and pain can all impede normal nesting behavior, making the model appropriate for detecting possible adverse reactions (Negus, 2019). In the experiment, nesting material (nestlets) was placed in six different zones of a mouse's cage. As the mouse makes its nest, it gathers all nestlets in a single zone (Negus et al., 2015). We measured the numbers of zones cleared over time. ST034307 did not disrupt nesting behaviors at doses up to 30 mg/kg compared to vehicle (**Figure 3A**). Morphine, on the other hand, caused a robust reduction of nesting behavior at 3 mg/kg (**Figures 3B**—two-way ANOVA, $p < 0.001$ and $p < 0.01$ at 30 and 60 min, respectively). Morphine's disruption of nesting behavior at the last time-point of the experiment resulted in an ED_{50} equal to 3.04 mg/kg [95% CI 1.16 to 11.32] (**Figure 3C**).

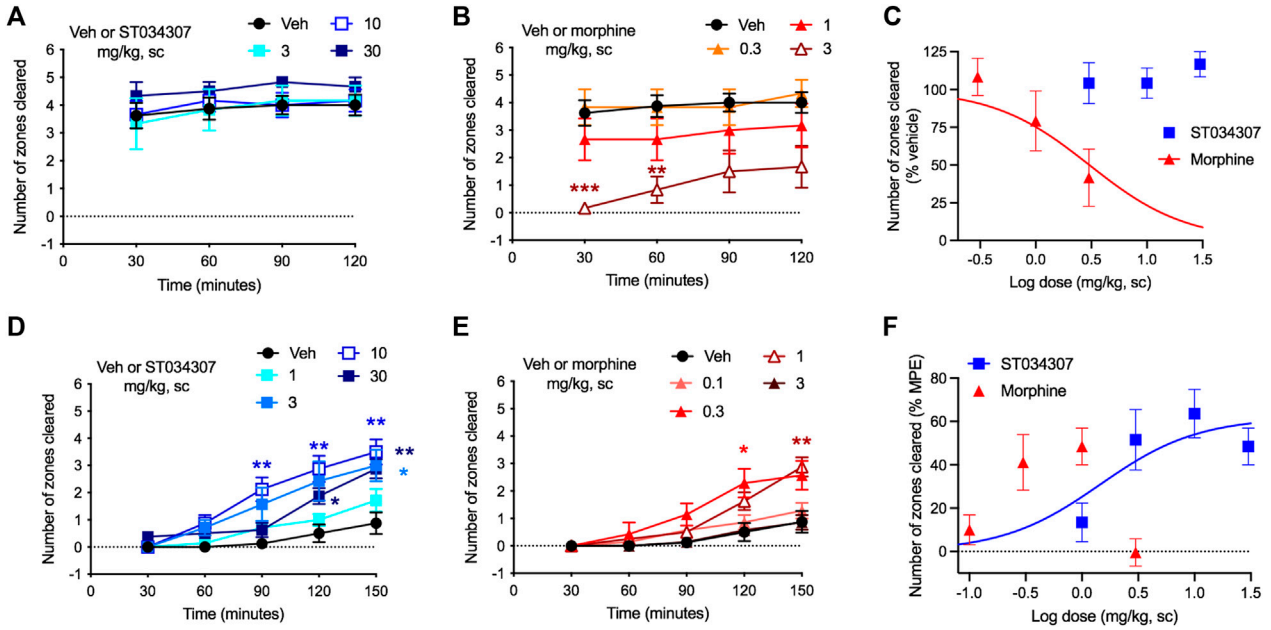

FIGURE 3 | ST034307 rescues acid-depressed mouse nesting behavior. **(A)** ST034307 did not reduce mouse nesting behavior at doses up to 30 mg/kg. **(B)** At a dose of 3 mg/kg, morphine significantly reduced mouse nesting behavior at 30 and 60 min after nesting measurements were started. **(C)** Dose-response curves of the last experimental timepoints the graphs in **(A)** and **(B)**. Vehicle's response was set as 100% and the maximal possible effect (0) to 0%. **(D)** and **(E)** 3 mg/kg, 10 mg/kg, and 30 mg/kg ST034307 and 0.3 mg/kg and 1 mg/kg morphine significantly rescued mouse nesting behavior that was reduced by an intraperitoneal injection of 1% lactic acid. **(F)** Dose-response curves of the last experimental timepoints from the graphs in **(D)** and **(E)**. Vehicle's response was set as 0% and the maximal possible effect (5) to 100%. Data in all graphs represent the average ±S.E.M., N = 6–8. $*p < 0.05$, $**p < 0.01$, $***p < 0.001$ in two-way ANOVA with Dunnett's test.

As pain can also disrupt nesting behavior, we next tested whether ST034307 could recover nesting in mice that were treated with 1% lactic acid intraperitoneally. Lactic acid treatment caused a profound reduction in nesting behavior (**Figures 3D,E**). Mice that were treated with 3, 10, or 30 mg/kg ST034307 displayed a significant increase in nesting behavior compared to vehicle-treated animals (**Figure 3D**). For morphine, 0.3 and 1 mg/kg caused a significant recovery of nesting behavior during the assay, while 0.1 and 3 mg/kg did not (**Figure 3E**). ST034307s recovery of nesting behavior at the last time-point of the experiment resulted in an ED_{50} equal to 1.45 mg/kg [95% CI 0.22 to 4.93] (**Figure 3F**). As the 3 mg/kg dose of morphine depressed mouse nesting, an ED_{50} value was not calculated for the compound (**Figure 3E**). The ED_{50} value and partial response of ST034307 in this experiment are consistent with what was observed in the acid-induced writhing assay (**Figure 2C**).

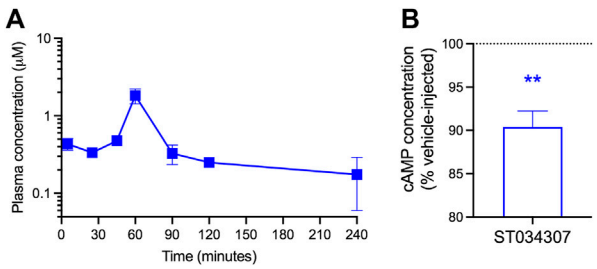

FIGURE 4 | ST034307 plasma concentration peaks at 60 min after subcutaneous injection and reduces cAMP concentration in the DRG. **(A)** Plasma ST0304307 concentration versus time profile after a single 10 mg/kg subcutaneous injection in mice. N = 2,3. **(B)** A 10 mg/kg subcutaneous injection of ST034307 causes a reduction in cAMP concentration in the DRG of mice. DRG were dissected 90 min after injection. Data was normalized to respective matched vehicle-injected controls. N = 6. $**p < 0.01$ in one sample T test compared to 100%.

3.4 ST034307 Reduces cAMP Concentration in Mouse DRG

Given the positive results from the nesting experiments, we decided to determine the concentrations of ST0340307 in plasma and brain of mice at different timepoints following a subcutaneous injection with a dose of 10 mg/kg (**Figure 4A**). A plasma concentration of 0.44 (±0.08) μM was observed immediately following the injection at 5 min. A sharp peak was present 60 min after the injection at 1.82 (±0.39) μM and after 90 min the plasma concentration dropped back to levels similar to the levels before the peak (0.33 μM ± 0.09). The half-life of ST0304307 was determined to be approximately 161 (±88) minutes and the compound was rapidly cleared (CL/F) from the body at a rate of 305.04 (±22.63) ml/min. ST0304307 may be highly tissue bound as its volume of distribution (V/F) of 1619 (±790) ml is much greater than the total body water volume (14.5 ml) of a 24 g (average weight) mouse (Davies and Morris, 1993). This type of distribution may also indicate extensive red

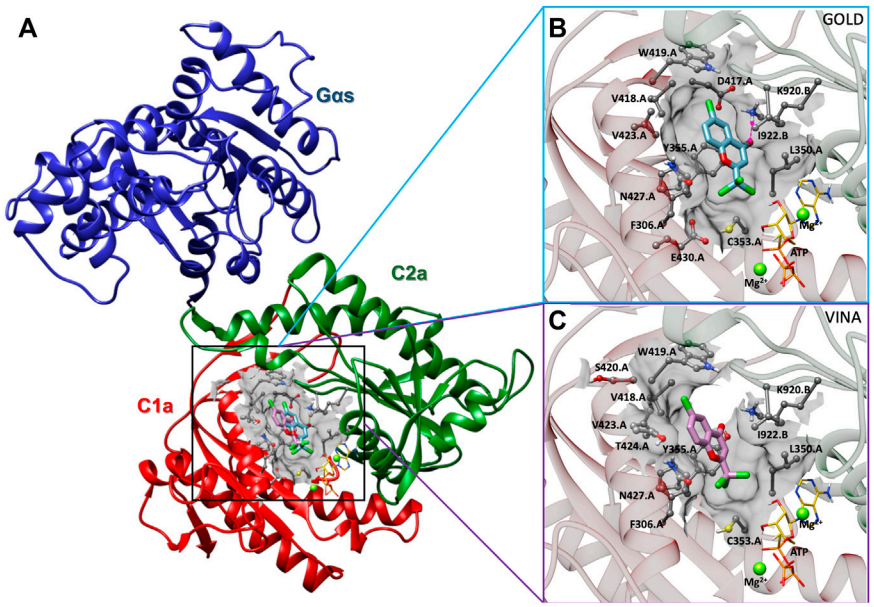

FIGURE 5 | Prediction of the interaction between AC1 and ST034307. **(A)** Cartoon representation of the AC1 model, showing its catalytic domain (C1a, in red, and C2a, in green) complexed to $G\alpha_s$ (in blue), ST034307 (in cyan or purple), ATP (in yellow), and two magnesium ions (Mg^{2+}, in green). Predicted poses of ST034307, using Gold **(B)** and Autodock Vina **(C)** programs, presenting hydrogen-bond (interrupted purple line) and steric interactions. The AC1 residue structures are shown as ball and stick models, ST034307 and ATP as stick models, and Mg^{2+} ions as sphere models using UCSF Chimera program (Pettersen et al., 2004). All the structures are colored by atom: the nitrogen atoms are shown in blue, the oxygen atoms in red, the chlorine atoms in green, the hydrogen atoms in white, and the carbon chain in gray, cyan, or purple. Non-polar hydrogens have been omitted for clarity.

blood cell uptake. To our surprise, none of the timepoints measured resulted in detectable levels of ST034307 in the brains of those mice.

As we were unable to detect ST034307 in mouse brain and AC1 is expressed in the DRG, we decided to determine if a subcutaneous injection of 10 mg/kg ST034307 would cause a reduction in cAMP concentration in mouse DRG. A 10% reduction in cAMP concentration was observed in the DRG of ST034307-injected mice in comparison to vehicle-matched controls (**Figure 4B**).

3.5 ST034307 Interacts With the Interface of C1a and C2a Domains of AC1

In order to determine the binding interaction of ST034307 with AC1, we constructed a molecular model of AC1. The results of PROCHECK's Ramachandran regions (**Supplementary Figure S1**), main-chain (**Supplementary Figure S2**), and side-chain parameters (**Supplementary Figure S3**), as well as VERIFY 3D (**Supplementary Figure S4**), and QMEANDisCo (**Supplementary Figure S5**) analyses indicated that the AC1 model was structurally valid to further computational studies. Thus, to predict the binding mode of ST034307 to AC1, we carried out molecular docking simulations using two programs, GOLD 2020.3.0 and Autodock Vina 1.1.2 (Jones et al., 1997; Trott and Olson, 2010). Although these programs present differences concerning their search algorithm and scoring function, the best-predicted poses resulting from the different programs showed similar binding modes (RMSD = 2.35Å) into the AC1 model (**Figure 5A**). The binding site was located into a cavity adjacent to the ATP binding pocket and between domains C1a and C2a, at the catalytic site interface. The best predicted pose for ST034307 presents a chemPLP score of 49.36 a. u, using the GOLD software, showing a hydrogen bond with the amine group from the side chain of Lys920 (C2a), and steric interactions with Phe306, Leu350, Cys353, Tyr355, Asp417, Val418, Trp419, Val423, Asn427, and Glu430 from C1a and with Lys920 and Ile922 from C2a (**Figure 5B**; **Supplementary Figure S6A**). Using Autodock Vina, the best-predicted pose for ST034307 presents an interaction energy value of −6.9 kcal/mol, showing only steric interactions with Phe306, Leu350, Cys353, Tyr355, Asp417, Val418, Trp419, Ser420, Val423, Thr224, and Asn427 from C1a and with Lys920 and Ile922 from C2a (**Figures 5C**; **Supplementary Figure S6B**).

4 DISCUSSION AND CONCLUSION

Previous studies using AC1-KO mice have indicated that inhibition of AC1 could be a new strategy to treat pain and opioid dependence (Wei et al., 2002; Vadakkan et al., 2006; Xu et al., 2008; Zachariou et al., 2008; Luo et al., 2013). Inspired by those studies, we discovered and characterized ST034307 (Brust et al., 2017). The compound displayed remarkable selectivity for inhibition of AC1 vs. all other membrane-bound AC isoforms. And while our previous manuscript focused on the molecular characterization of ST034307, we also showed that the compound relieves pain in a mouse model of CFA-induced allodynia (Brust

et al., 2017). Here, those findings were expanded in multiple different ways.

First, we focused on the activity of the compound in two different models of pain-induced behaviors. In the first, intraplantar injections with formalin to the hind paws of the mice induce a paw licking behavior that is reflective of pain (Tjolsen et al., 1992). The experiment is divided into two distinct phases. The first phase, which includes the first 10 min, represents chemical nociception due to the action of formalin on primary afferent nerve fibers (Mcnamara et al., 2007). ST034307 had no effects on that phase of the experiment (**Figure 1C**). This is consistent with our results with AC1-KO mice (**Figure 1E**) and with a previous study that showed that AC1-KO mice do not have increased thresholds to thermal, mechanical, or chemical acute nociception compared to wild-type mice (Wei et al., 2002). Morphine, in contrast, reduced chemical nociception in both wild-type and AC1-KO mice in a manner that is consistent with the activation of the mu opioid receptor (MOR). Activation of the MOR induces inhibition of AC isoforms as well as modulation of ion channels through Gβγ subunits (Raehal et al., 2011). MOR-induced activation of G protein-coupled inwardly rectifying potassium channels (GIRK) and inhibition of voltage-gated calcium channels induces neuronal hyperpolarization and a reduction of neurotransmission that is consistent with morphine's effects on acute nociception assays (Raehal et al., 2011).

The formalin-induced paw licking behavior between minutes 16 and 40 is believed to be caused by the development of an inflammatory reaction that induces nerve sensitization (Woolf, 1983; Tjolsen et al., 1992; Negus, 2019). This process involves the strengthening of synaptic connections through LTP and requires cAMP (Ferguson and Storm, 2004; Latremoliere and Woolf, 2009; Sharif-Naeini and Basbaum, 2011; Zhuo, 2012). As expected, ST034307 caused a reduction in licking behavior during that phase. A reduction of formalin-induced paw licking during that phase was also observed in AC1-KO mice compared to wild-type animals. These data are consistent with previous work showing that AC1-KO mice have an increased threshold to inflammatory pain and indicate a possible use of selective AC1 inhibitors to treat this type of pain (Wei et al., 2002). As previously reported, morphine was also efficacious in this model (Pantouli et al., 2021). Morphine's higher potency in this phase of the experiment compared to its potency for reducing chemical nociception may be explained by the combination of the MOR's effects on G proteins, namely inhibition of ACs and activation of GIRK.

Next, we showed that ST034307 decreases the number of abdominal constrictions (writhing) in mice injected intraperitoneally with acetic acid. Intraperitoneal injections with irritant agents cause peritovisceral pain and previous studies suggest that all analgesics can reduce writhing in this model (Collier et al., 1968; Negus, 2019). In contrast to morphine, ST034307 did not result in the maximal possible effect in this experiment, an outcome that was mimicked by AC1-KO mice. This partial response allowed us to further confirm that the effect of ST034307 in this model was through AC1 inhibition, as morphine, but not ST034307, further reduced the number of acid-induced abdominal constrictions in AC1-KO mice (**Figure 2D**).

The use of analgesic agents often requires chronic dosing, which may last days, months, or even years depending on the patient's condition. Unfortunately, chronic analgesic dosing may lead to analgesic tolerance (Stein, 2016). Opioid tolerance is well documented in humans and rodents, and results in a loss of analgesic efficacy over time (Raehal et al., 2011; Stein, 2016; Grim et al., 2020). At the molecular level, it has been proposed that opioid tolerance is caused by agonist-induced recruitment of βarrestins to the MOR. βarrestins induce receptor internalization (removal from the membrane) and, therefore, reduce the pool of available receptors for opioid action (Raehal et al., 2011). As ST034307 acts as an inhibitor of AC1, the mechanisms commonly linked to tolerance (receptor downregulation) should not be present. Consistently, we did not observe any tolerance to a high daily dose of ST034307 for up to 8 days in the mouse acid-induced writhing assay. This is in contrast to morphine, which displayed a marked reduction of analgesic efficacy, consistent with analgesic tolerance. As the two compounds act through different mechanisms (though the MOR inhibits AC1) (Brust et al., 2017), there was no observable development of cross-tolerance.

Paw licking and abdominal constrictions are examples of pain-stimulated behaviors. While useful in pain studies, a reduction of these behaviors may not necessarily indicate pain relief. Compounds that induce paralysis, sedation, or stimulate a competing behavior, for instance, can still cause a marked reduction of behavior in those experiments, but are not necessarily relieving pain (Negus et al., 2015; Negus, 2019). Therefore, we have employed the pain-depressed behavior of nesting as another method to determine the analgesic efficacy of ST034307. Different types of stimuli (such as pain, stress, and sedation) can cause disruptions of mouse innate behaviors. Therefore, in order for a compound to display pain relief in this model, it may not present disruptive properties, as if it does, nesting behavior will be further reduced (see the 3 mg/kg dose of morphine in **Figures 3C,E**) (Negus et al., 2015). ST034307 did not disrupt nesting behavior at doses up to 30 mg/kg, indicating good tolerability in this model. Furthermore, all doses that were effective at relieving pain in the previous models, also significantly recovered nesting behavior that was reduced by an intraperitoneal injection of lactic acid (**Figure 3D**). According to Negus (2019), the combination of the results from our nesting experiments and our pain-stimulated behavior experiments makes ST034307 (and possibly other AC1-selective inhibitors) a "high-priority" analgesic compound for "further testing" (Negus, 2019).

While the nesting experiments provide a measure of safety, studies describing the full spectrum of possible adverse reactions that result from AC1 inhibition are still needed. The high expression levels of AC1 in the hippocampus suggests that the initial focus of these studies should be on learning and memory. ST034307 is selective for AC1 vs. AC8. Nevertheless, AC1-KO mice still display impaired performance in certain learning and memory tasks (Shan et al., 2008; Zheng et al., 2016; Brust et al.,

2017). The use of a pharmacological agent will allow us to determine if those effects are a result of developmental issues (as AC1 expression is important for synaptic plasticity and development) (Haupt et al., 2010; Wang et al., 2011) or if there is an acute dose-dependent effect. If ST034307 is to be used for those experiments, intrathecal or intracerebroventricular injections will be required to ensure that the compound reaches the brain. The development of chronic adverse effects, other than analgesic tolerance, should also be investigated. It is not expected that AC1 inhibitors will be rewarding, but the current state of the opioid crisis indicates that this should be tested experimentally, and the effects of AC1 inhibitors on the release of dopamine in the nucleus accumbens should also be assessed.

It is noteworthy that the current experiments were performed with subcutaneous injections, instead of the intrathecal injections from Brust et al., 2017. This allowed us to determine the disposition of the compound in plasma and brain. The plasma concentration of ST034307 peaked 1 h after injection. Notably, we were unable to detect ST034307 in the brain. Nevertheless, the disposition of this compound in plasma indicates a wide distribution in the body and rapid clearance resulting in relatively low concentrations compared to the administered dose. These concentrations persist for at least 4 h to account for the effects that are seen in these experiments.

A recent study reported that the DRG is an important site for the role AC1 plays in pain and nociception (Johnson et al., 2020). This is related to the requirement of cAMP for central sensitization (Ferguson and Storm, 2004; Zhuo, 2012). Accordingly, we observed a reduction in cAMP concentrations in the DRG of mice injected with ST034307 compared to vehicle-matched controls. It should be noted that the DRG homogenates used in our experiments contain different cell types in addition to the peripheral sensory pain afferents, hence the relatively small reduction in cAMP observed. In addition, the decrease in cAMP concentration observed in the DRG does not prevent the involvement of other sites not examined in the present study in ST034307s effects. The fact that ST034307 appears not to reach the brain also precludes the compound's activity in the hippocampus and makes it unlikely that this particular compound, when administered subcutaneously, would cause adverse effects related to learning and memory.

In the last set of data presented in the manuscript, the interaction between ST034307 and AC1 was mapped using molecular docking. Those results, achieved using two different programs, suggest that ST034307 interacts at a site located between the ATP and forskolin binding sites. This binding site is located at the interface of the C1a and C2a domains and is indicative of a mixed or uncompetitive mechanism. The action of ST034307 is proposed to cause a disruption of the structure of AC1's catalytic domain and, consequently, enzymatic inhibition. As our modeling showed that ST034307 does not bind to the ATP binding site, it is consistent with our previous findings that indicate that the compound is not a P-site inhibitor (Brust et al., 2017; Dessauer et al., 2017).

As encouraging as the data presented in the manuscript appears, other compounds that looked promising in pre-clinical models of pain have failed to translate to clinic (Negus, 2019). While the nesting experiments account for some adverse effects and competing behaviors that may generate false positives, additional studies on ST034307 and the class of AC1 inhibitors are still needed. Particular attention should be devoted to possible impairments on learning and memory as well as other models of pain that reflect pain states that are different from the ones already examined. Experiments with AC1 inhibitors that can reach the brain are also desired. Nevertheless, the present work clearly demonstrates a correlation between selective inhibition of AC1 and behaviors that are consistent with analgesia in mice. More work is still needed to establish this class of compounds as novel pain therapeutics; however, the present study represents an important step that may signal that selective AC1 inhibitors should be prioritized for further testing and advancement for the treatment of pain.

DATA AVAILABILITY STATEMENT

The datasets presented in this study can be found in online repositories. The names of the repository/repositories and accession number(s) can be found in the article/ **Supplementary Material**.

ETHICS STATEMENT

The animal study was reviewed and approved by the Institutional Animal Care and Use Committee (IACUC) of Palm Beach Atlantic University, protocol number 2020-01AMOUSE approved on 10 January 2020.

AUTHOR CONTRIBUTIONS

Conceptualization: TB. Experimental design: TB, GG, AN, LH. Performed experiments: TB, GG, TP, LH, AS, SC, KV, TA, VS. Data analyses: TB, LH, AN. Provided needed equipment or materials: NB, HW. Writing: TB wrote the first draft of the manuscript and all authors contributed, reviewed, and edited.

FUNDING

This work is supported by the American Association of Colleges of Pharmacy's New Investigator Award (TB), the Lloyd L. Gregory School of Pharmacy's IntegraConnect grant (TB and AN), Palm Beach Atlantic University's Quality Initiative grant (TB), Fundação Carlos Chagas Filho de Amparo à Pesquisa do Estado do Rio de Janeiro (FAPERJ) (NB), Conselho Nacional de Desenvolvimento Científico e Tecnológico (CNPq), Fundação de Apoio à Fiocruz (FIOTEC) (NB), Coordenação de

Aperfeiçoamento de Pessoal de Nível Superior (CAPES)—Finance Code 001 (NB), and Programa Nacional de Apoio ao Desenvolvimento da Metrologia, Qualidade e Tecnologia (PRONAMETRO) from Instituto Nacional de Metrologia, Qualidade e Tecnologia (INMETRO) (TA).

SUPPLEMENTARY MATERIAL

The Supplementary Material for this article can be found online at: https://www.frontiersin.org/articles/10.3389/fphar.2022.935588/full#supplementary-material

REFERENCES

Altschul, S. F., Gish, W., Miller, W., Myers, E. W., and Lipman, D. J. (1990). Basic Local Alignment Search Tool. *J. Mol. Biol.* 215, 403–410. doi:10.1016/S0022-2836(05)80360-2

Berman, H. M., Battistuz, T., Bhat, T. N., Bluhm, W. F., Bourne, P. E., Burkhardt, K., et al. (2002). The Protein Data Bank. *Acta Crystallogr. D. Biol. Crystallogr.* 58, 899–907. doi:10.1107/s0907444902003451

Brand, C. S., Hocker, H. J., Gorfe, A. A., Cavasotto, C. N., and Dessauer, C. W. (2013). Isoform Selectivity of Adenylyl Cyclase Inhibitors: Characterization of Known and Novel Compounds. *J. Pharmacol. Exp. Ther.* 347, 265–275. doi:10.1124/jpet.113.208157

Brust, T. F., Alongkronrusmee, D., Soto-Velasquez, M., Baldwin, T. A., Ye, Z., Dai, M., et al. (2017). Identification of a Selective Small-Molecule Inhibitor of Type 1 Adenylyl Cyclase Activity with Analgesic Properties. *Sci. Signal* 10, 5381. doi:10.1126/scisignal.aah5381

Brust, T. F., Conley, J. M., and Watts, V. J. (2015). Gα(i/o)-coupled Receptor-Mediated Sensitization of Adenylyl Cyclase: 40 Years Later. *Eur. J. Pharmacol.* 763, 223–232. doi:10.1016/j.ejphar.2015.05.014

Brust, T. F., Morgenweck, J., Kim, S. A., Rose, J. H., Locke, J. L., Schmid, C. L., et al. (2016). Biased Agonists of the Kappa Opioid Receptor Suppress Pain and Itch without Causing Sedation or Dysphoria. *Sci. Signal* 9, ra117. doi:10.1126/scisignal.aai8441

Collier, H. O., Dinneen, L. C., Johnson, C. A., and Schneider, C. (1968). The Abdominal Constriction Response and its Suppression by Analgesic Drugs in the Mouse. *Br. J. Pharmacol. Chemother.* 32, 295–310. doi:10.1111/j.1476-5381.1968.tb00973.x

Colovos, C., and Yeates, T. O. (1993). Verification of Protein Structures: Patterns of Nonbonded Atomic Interactions. *Protein Sci.* 2, 1511–1519. doi:10.1002/pro.5560020916

Cooper, D. M., and Crossthwaite, A. J. (2006). Higher-order Organization and Regulation of Adenylyl Cyclases. *Trends Pharmacol. Sci.* 27, 426–431. doi:10.1016/j.tips.2006.06.002

Cumbay, M. G., and Watts, V. J. (2001). Heterologous Sensitization of Recombinant Adenylate Cyclases by Activation of D(2) Dopamine Receptors. *J. Pharmacol. Exp. Ther.* 297 (293), 1201

Davies, B., and Morris, T. (1993). Physiological Parameters in Laboratory Animals and Humans. *Pharm. Res.* 10, 1093–1095. doi:10.1023/a:1018943613122

Dessauer, C. W., Watts, V. J., Ostrom, R. S., Conti, M., Dove, S., and Seifert, R. (2017). International Union of Basic and Clinical Pharmacology. CI. Structures and Small Molecule Modulators of Mammalian Adenylyl Cyclases. *Pharmacol. Rev.* 69, 93–139. doi:10.1124/pr.116.013078

Ferguson, G. D., and Storm, D. R. (2004). Why Calcium-Stimulated Adenylyl Cyclases? *Physiol. (Bethesda)* 19, 271–276. doi:10.1152/physiol.00010.2004

Grim, T. W., Schmid, C. L., Stahl, E. L., Pantouli, F., Ho, J. H., Acevedo-Canabal, A., et al. (2020). A G Protein Signaling-Biased Agonist at the μ-opioid Receptor Reverses Morphine Tolerance while Preventing Morphine Withdrawal. *Neuropsychopharmacology* 45, 416–425. doi:10.1038/s41386-019-0491-8

Haupt, C., Langhoff, J., and Huber, A. B. (2010). Adenylate Cyclase 1 Modulates Peripheral Nerve Branching Patterns. *Mol. Cell Neurosci.* 45, 439–448. doi:10.1016/j.mcn.2010.08.003

Humphrey, W., Dalke, A., and Schulten, K. (1996). VMD: Visual Molecular Dynamics. *J. Mol. Graph* 14 (33-38), 33–38. doi:10.1016/0263-7855(96)00018-5

Johnson, K., Doucette, A., Edwards, A., Watts, V. J., and Klein, A. H. (2020). *Reduced Activity of Adenylyl Cyclase 1 Attenuates Morphine Induced Hyperalgesia and Inflammatory Pain in Mice*. Cold Spring Harbor: Cold Spring Harbor Laboratory.

Jones, G., Willett, P., Glen, R. C., Leach, A. R., and Taylor, R. (1997). Development and Validation of a Genetic Algorithm for Flexible Docking. *J. Mol. Biol.* 267, 727–748. doi:10.1006/jmbi.1996.0897

Kaur, J., Soto-Velasquez, M., Ding, Z., Ghanbarpour, A., Lill, M. A., Van Rijn, R. M., et al. (2018). Optimization of a 1,3,4-oxadiazole Series for Inhibition of Ca2+/calmodulin-Stimulated Activity of Adenylyl Cyclases 1 and 8 for the Treatment of Chronic Pain. *Eur. J. Med. Chem.* 162, 568–585. doi:10.1016/j.ejmech.2018.11.036

Laskowski, R. A., Macarthur, M. W., Moss, D. S., and Thornton, J. M. (1993). PROCHECK: a Program to Check the Stereochemical Quality of Protein Structures. *J. Appl. Cryst.* 26, 283–291. doi:10.1107/s0021889892009944

Latremoliere, A., and Woolf, C. J. (2009). Central Sensitization: a Generator of Pain Hypersensitivity by Central Neural Plasticity. *J. Pain* 10, 895–926. doi:10.1016/j.jpain.2009.06.012

Luo, J., Phan, T. X., Yang, Y., Garelick, M. G., and Storm, D. R. (2013). Increases in cAMP, MAPK Activity, and CREB Phosphorylation during REM Sleep: Implications for REM Sleep and Memory Consolidation. *J. Neurosci.* 33, 6460–6468. doi:10.1523/JNEUROSCI.5018-12.2013

Masada, N., Schaks, S., Jackson, S. E., Sinz, A., and Cooper, D. M. (2012). Distinct Mechanisms of Calmodulin Binding and Regulation of Adenylyl Cyclases 1 and 8. *Biochemistry* 51, 7917–7929. doi:10.1021/bi300646y

Mcnamara, C. R., Mandel-Brehm, J., Bautista, D. M., Siemens, J., Deranian, K. L., Zhao, M., et al. (2007). TRPA1 Mediates Formalin-Induced Pain. *Proc. Natl. Acad. Sci. U. S. A.* 104, 13525–13530. doi:10.1073/pnas.0705924104

Mistry, J., Chuguransky, S., Williams, L., Qureshi, M., Salazar, G. A., Sonnhammer, E. L. L., et al. (2021). Pfam: The Protein Families Database in 2021. *Nucleic Acids Res.* 49, D412–D419. doi:10.1093/nar/gkaa913

Negus, S. S. (2019). Core Outcome Measures in Preclinical Assessment of Candidate Analgesics. *Pharmacol. Rev.* 71, 225–266. doi:10.1124/pr.118.017210

Negus, S. S., Neddenriep, B., Altarifi, A. A., Carroll, F. I., Leitl, M. D., and Miller, L. L. (2015). Effects of Ketoprofen, Morphine, and Kappa Opioids on Pain-Related Depression of Nesting in Mice. *Pain* 156, 1153–1160. doi:10.1097/j.pain.0000000000000171

Ostrom, K. F., Lavigne, J. E., Brust, T. F., Seifert, R., Dessauer, C. W., Watts, V. J., et al. (2022). Physiological Roles of Mammalian Transmembrane Adenylyl Cyclase Isoforms. *Physiol. Rev.* 102, 815–857. doi:10.1152/physrev.00013.2021

Pantouli, F., Grim, T. W., Schmid, C. L., Acevedo-Canabal, A., Kennedy, N. M., Cameron, M. D., et al. (2021). Comparison of Morphine, Oxycodone and the Biased MOR Agonist SR-17018 for Tolerance and Efficacy in Mouse Models of Pain. *Neuropharmacology* 185, 108439. doi:10.1016/j.neuropharm.2020.108439

Pettersen, E. F., Goddard, T. D., Huang, C. C., Couch, G. S., Greenblatt, D. M., Meng, E. C., et al. (2004). UCSF Chimera-Aa Visualization System for Exploratory Research and Analysis. *J. Comput. Chem.* 25, 1605–1612. doi:10.1002/jcc.20084

Raehal, K. M., Schmid, C. L., Groer, C. E., and Bohn, L. M. (2011). Functional Selectivity at the μ-opioid Receptor: Implications for Understanding Opioid Analgesia and Tolerance. *Pharmacol. Rev.* 63, 1001–1019. doi:10.1124/pr.111.004598

Sali, A., and Blundell, T. L. (1993). Comparative Protein Modelling by Satisfaction of Spatial Restraints. *J. Mol. Biol.* 234, 779–815. doi:10.1006/jmbi.1993.1626

Shan, Q., Chan, G. C., and Storm, D. R. (2008). Type 1 Adenylyl Cyclase Is Essential for Maintenance of Remote Contextual Fear Memory. *J. Neurosci.* 28, 12864–12867. doi:10.1523/JNEUROSCI.2413-08.2008

Sharif-Naeini, R., and Basbaum, A. I. (2011). Targeting Pain where it Resides In the Brainthe Brain. *Sci. Transl. Med.* 3, 65ps1. doi:10.1126/scitranslmed.3002077

Sleigh, J. N., West, S. J., and Schiavo, G. (2020). A Video Protocol for Rapid Dissection of Mouse Dorsal Root Ganglia from Defined Spinal Levels. *BMC Res. Notes* 13, 302. doi:10.1186/s13104-020-05147-6

Stein, C. (2016). Opioid Receptors. *Annu. Rev. Med.* 67, 433–451. doi:10.1146/annurev-med-062613-093100

Studer, G., Rempfer, C., Waterhouse, A. M., Gumienny, R., Haas, J., and Schwede, T. (2020). Qmeandisco-Distance Constraints Applied on Model Quality Estimation. *Bioinformatics* 36, 1765–1771. doi:10.1093/bioinformatics/btz828

Tarselli, M. A., Raehal, K. M., Brasher, A. K., Streicher, J. M., Groer, C. E., Cameron, M. D., et al. (2011). Synthesis of Conolidine, a Potent Non-Opioid Analgesic for Tonic and Persistent Pain. *Nat. Chem.* 3, 449–453. doi:10.1038/nchem.1050

Tjølsen, A., Berge, O. G., Hunskaar, S., Rosland, J. H., and Hole, K. (1992). The Formalin Test: An Evaluation of the Method. *Pain* 51, 5–17. doi:10.1016/0304-3959(92)90003-t

Trott, O., and Olson, A. J. (2010). Autodock Vina: Improving the Speed and Accuracy of Docking With a New Scoring Function, Efficient Optimization, and Multithreading. *J. Comput. Chem.* 31, 455–461. doi:10.1002/jcc.21334

Uniprot, C. (2021). Uniprot: The Universal Protein Knowledgebase in 2021. *Nucleic Acids Res.* 49, D480–D489. doi:10.1093/nar/gkaa1100

Vadakkan, K. I., Wang, H., Ko, S. W., Zastepa, E., Petrovic, M. J., Sluka, K. A., et al. (2006). Genetic Reduction of Chronic Muscle Pain in Mice Lacking Calcium/Calmodulin-Stimulated Adenylyl Cyclases. *Mol. Pain* 2, 7. doi:10.1186/1744-8069-2-7

Wang, H., Liu, H., Storm, D. R., and Zhang, Z. W. (2011). Adenylate Cyclase 1 Promotes Strengthening and Experience-Dependent Plasticity of Whisker Relay Synapses in the Thalamus. *J. Physiol.* 589, 5649–5662. doi:10.1113/jphysiol.2011.213702

Wang, H., Pineda, V. V., Chan, G. C., Wong, S. T., Muglia, L. J., and Storm, D. R. (2003). Type 8 Adenylyl Cyclase is Targeted to Excitatory Synapses and Required for Mossy Fiber Long-Term Potentiation. *J. Neurosci.* 23, 9710–9718. doi:10.1523/jneurosci.23-30-09710.2003

Wei, F., Qiu, C. S., Kim, S. J., Muglia, L., Maas, J. W., Pineda, V. V., et al. (2002). Genetic Elimination of Behavioral Sensitization in Mice Lacking Calmodulin-Stimulated Adenylyl Cyclases. *Neuron* 36, 713–726. doi:10.1016/s0896-6273(02)01019-x

Wei, F., Vadakkan, K. I., Toyoda, H., Wu, L. J., Zhao, M. G., Xu, H., et al. (2006). Calcium Calmodulin-Stimulated Adenylyl Cyclases Contribute to Activation of Extracellular Signal-Regulated Kinase in Spinal Dorsal Horn Neurons in Adult Rats and Mice. *J. Neurosci.* 26, 851–861. doi:10.1523/JNEUROSCI.3292-05.2006

Wong, S. T., Athos, J., Figueroa, X. A., Pineda, V. V., Schaefer, M. L., Chavkin, C. C., et al. (1999). Calcium-Stimulated Adenylyl Cyclase Activity is Critical for Hippocampus-Dependent Long-Term Memory and Late Phase LTP. *Neuron* 23, 787–798. doi:10.1016/s0896-6273(01)80036-2

Woolf, C. J. (1983). Evidence for a Central Component of Post-Injury Pain Hypersensitivity. *Nature* 306, 686–688. doi:10.1038/306686a0

Xu, H., Wu, L. J., Wang, H., Zhang, X., Vadakkan, K. I., Kim, S. S., et al. (2008). Presynaptic and Postsynaptic Amplifications of Neuropathic Pain in the Anterior Cingulate Cortex. *J. Neurosci.* 28, 7445–7453. doi:10.1523/JNEUROSCI.1812-08.2008

Yang, J., and Zhang, Y. (2015). I-TASSER Server: New Development for Protein Structure and Function Predictions. *Nucleic Acids Res.* 43, W174–W181. doi:10.1093/nar/gkv342

Zachariou, V., Liu, R., Laplant, Q., Xiao, G., Renthal, W., Chan, G. C., et al. (2008). Distinct Roles of Adenylyl Cyclases 1 and 8 in Opiate Dependence: Behavioral, Electrophysiological, and Molecular Studies. *Biol. Psychiatry* 63, 1013–1021. doi:10.1016/j.biopsych.2007.11.021

Zheng, F., Zhang, M., Ding, Q., Sethna, F., Yan, L., Moon, C., et al. (2016). Voluntary Running Depreciates the Requirement of Ca^{2+}-Stimulated Camp Signaling in Synaptic Potentiation and Memory Formation. *Learn Mem.* 23, 442–449. doi:10.1101/lm.040642.115

Zhuo, M. (2012). Targeting Neuronal Adenylyl Cyclase for the Treatment of Chronic Pain. *Drug Discov. Today* 17, 573–582. doi:10.1016/j.drudis.2012.01.009

Conflict of Interest: The authors declare that the research was conducted in the absence of any commercial or financial relationships that could be construed as a potential conflict of interest.

Publisher's Note: All claims expressed in this article are solely those of the authors and do not necessarily represent those of their affiliated organizations, or those of the publisher, the editors and the reviewers. Any product that may be evaluated in this article, or claim that may be made by its manufacturer, is not guaranteed or endorsed by the publisher.